Spatial Distributions of Cold and Warm Interstellar Dust in M101 Resolved with AKARI/Far-Infrared Surveyor (FIS)

Toyoaki Suzuki[1], Hidehiro Kaneda[1], Takao Nakagawa[1], Sin'itirou Makiuti[1], Yoko Okada[1], Hiroshi Shibai[2], Mitsunobu Kawada[2], and Yasuo Doi[3]

ABSTRACT

The nearby face-on spiral galaxy M101 has been observed with the Far-Infrared Surveyor (FIS) onboard AKARI. The far-infrared four-band images reveal fine spatial structures of M101, which include global spiral patterns, giant HII regions embedded in outer spiral arms, and a bar-like feature crossing the center. The spectral energy distribution of the whole galaxy shows the presence of the cold dust component (18^{+4}_{-10} K) in addition to the warm dust component (55^{+9}_{-25} K). The distribution of the cold dust is mostly concentrated near the center, and exhibits smoothly distributed over the entire extent of the galaxy, whereas the distribution of the warm dust indicates some correlation with the spiral arms, and has spotty structures such as four distinctive bright spots in the outer disk in addition to a bar-like feature near the center tracing the CO intensity map. The star-formation activity of the giant HII regions that spatially correspond to the former bright spots is found to be significantly higher than that of the rest of the galaxy. Unlike our Galaxy, M101 is a peculiar normal galaxy with extraordinary active star-forming regions.

Subject headings: galaxies: ISM — infrared: galaxies — infrared: ISM — ISM: dust, extinction — ISM: structure

[1]Institute of Space and Astronautical Science, Japan Aerospace Exploration Agency, 3–1–1 Yoshinodai, Sagamihara-shi, Kanagaawa 229–8510

[2]Graduate School of Science, Nagoya University, Furu-cho, Chikusa-ku, Nagoya 464–8602

[3]Department of Earth Science and Astronomy, University of Tokyo, 3–8–1 Komaba, Megro-ku, Tokyo 153–8902

1. Introduction

The characteristics of large-scale star formation are of great importance to understand the evolution of a galaxy. One of the open fundamental questions is the dependence of the global star formation rate (SFR) on the total gas content of a galaxy. Far-infrared (IR) dust emission can provide us with reliable estimates of SFR. In general, spiral galaxies have cold and warm dust, as first suggested by de Jong et al. (1984), and confirmed by ISO observations (see review of Sauvage et al. 2005 and references therein). The cold dust component ($T_{\rm d}$ = 10–20 K) is associated with molecular and atomic hydrogen clouds, which is heated mostly by the general interstellar radiation field (ISRF) (Cox & Mezger 1989). The cold dust accounts for more than 90 % of the total interstellar dust in mass, and can therefore be used to estimate the total gas distribution over a galaxy. The contribution of the warm dust component ($T_{\rm d}$ = 25–40 K) can be used to estimate the SFR of massive stars ($\gtrsim$4 $M_{\odot}$); since the warm dust component is heated by O and early B stars in HII regions (Cox & Mezger 1989), its luminosity can reasonably be considered to reflect the SFR of massive stars, providing that the escape fraction of non-ionising UV photons from the HII regions is properly taken into account(Popescu & Tuffs 2005; Hippelein 2003). Hence, to properly address the question about the relation between the global SFR and the total gas content in spiral galaxies, it is crucial to separate the contributions of the cold and warm dust components and to discuss the spatially-resolved distribution of each component within a galaxy. Particularly for late-type spiral and irregular galaxies, most of the far-IR luminosity is carried by the cold dust primarily emitting longwards of the IRAS limit of 120 μm, and thus observations at wavelengths longer than 120 μm are essential to detect the cold dust component(Popescu et al. 2002; Vlahakis, et al. 2005).

Here we present new far-IR images of the nearby galaxy M101 obtained with the Far-Infrared Surveyor (FIS; Kawada et al. 2007) onboard AKARI (Murakami et al. 2007). M101 is a face-on spiral galaxy with global spiral patterns, classified as Sc(s)I (Sandage et al. 1981) with a distance of 7.4 Mpc (Jurcevic & Butcher 2006). The galaxy is an excellent candidate for this study, since it has a large optical size of 28×28 arcmin^2(Nilson 1973), well-developed spiral arms, and several conspicuous giant HII regions (NGC 5447, 5455, 5461, 5462, and 5471).

2. Observations

The observations were performed as part of the FIS calibration program on June 14th in 2006 by using one of the FIS observation modes, FIS01. The FIS was operated in a photometry mode with the four bands: N60 (65 μm), WIDE-S (90 μm), WIDE-L (140 μm), and N160 (160 μm).

3. Results

Figure 1 represents the far-IR four-band images of M101. The conspicuous four bright spots spatially correspond to the four giant HII regions, NGC 5447, 5455, 5461, and 5462, and they are even more emphatic in the WIDE-S and N60 band images. Among them, NGC 5461, which is located at 4.5 arcmin south-east from the center is brightest and even brighter than the center. Furthermore, as seen in the ISO 100 μm image(Tuffs & Gabriel 2003), a bar-like feature crossing the center can also be seen in the WIDE-S and N60 band images, which have striking resemblance to the distribution of CO emission (Kenney et al. 1991).

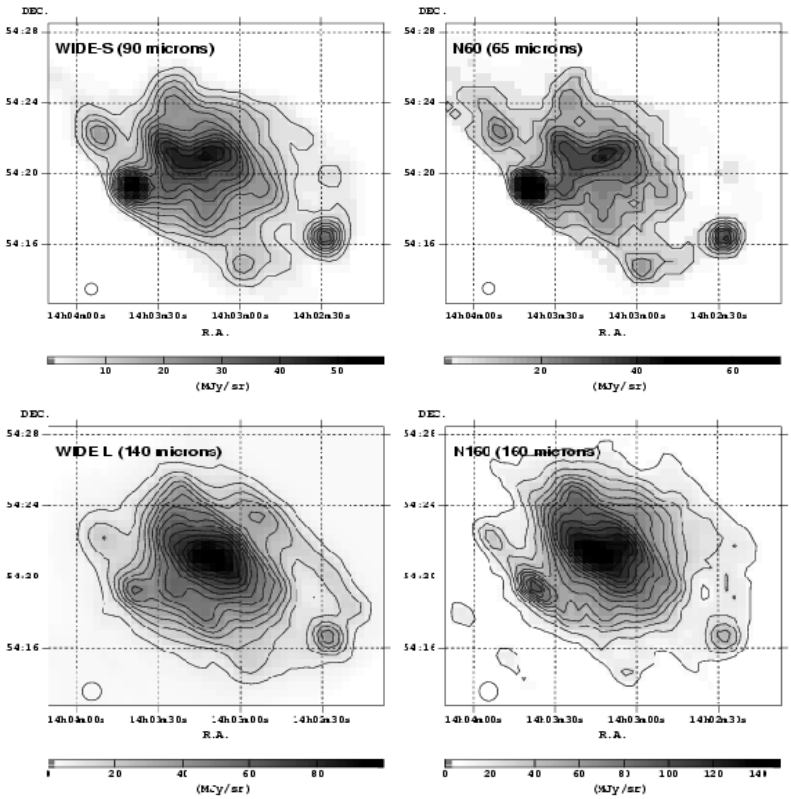

Fig. 1.— Four-band images of M101 in the WIDE-S (top-left), N60 (top-right), WIDE-L (bottom-left), and N160 (bottom-right) bands (Suzuki et al. 2007). The center wavelengths of the four bands are 65 μm for N60, 90 μm for WIDE-S, 140 μm for WIDE-L, and 160 μm for N160.

The spectral energy distribution (SED) of the whole galaxy is obtained by integrating the surface brightness. Figure 2 shows the resultant SED of M101. We have then fitted the AKARI and ISO data with a double-temperature blackbody model modified by an emissivity power-law index of 1. The best-fit temperatures of cold ($T_{\rm c}$) and warm ($T_{\rm w}$) dust components

are 18^{+4}_{-9} K and 55^{+9}_{-25} K, respectively. By using the best-fit double temperature modified blackbody model, the total far-IR luminosity ($L_{\rm FIR}$) of the galaxy is $(2.1^{+0.5}_{-0.4})\times10^{10}$ $L_\odot$. Hence, $L_{\rm FIR}/M_{\rm gas}$ is estimated to be 0.9 $L_\odot/M_\odot$ with the total gas mass ($M_{\rm H_2}$+$M_{\rm H_I}$) of 2.4×10^{10} $M_\odot$ (Kenney et al. 1991; Allen et al. 1973). According to Siebenmorgen, Krügel, & Chini (1999), by taking into account the presence of the cold dust component as well as the small $L_{\rm FIR}/M_{\rm gas}$ value, M101 can be classified as a normal galaxy.

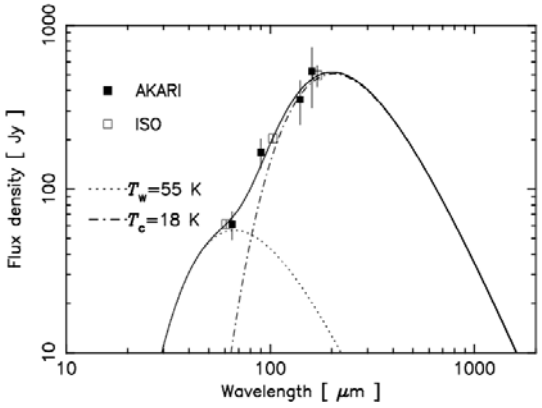

Fig. 2.— Spectral energy distribution of M101, together with the best-fit double-temperature modified blackbody model (Suzuki et al. 2007). Filled boxes represent the integrated flux densities in the FIS four bands, while open boxes correspond to those in the ISOPHOT far-IR bands (Tuffs & Gabriel 2003).

In order to derive the distributions of the cold and warm dust components in the galaxy, the spatial resolutions of the WIDE-S and N60 images are reduced to match those of the WIDE-L and N160 images by convolving the former images with a Gaussian kernel with the width of 20 arcsec, which has been performed before smoothing the images in figure 1. The images are then resized with the common spatial scale among the four bands: 25×25 arcsec^2. The flux densities at each image bin are derived from the aperture radius of 14 arcsec with the aperture-correction factors of 0.30 for the four bands. An individual SED constructed from the four-band fluxes at each image bin is then fitted with a two-temperature model, in which the temperatures are fixed at the values obtained for the SED of the whole galaxy. Figure 3 shows the distributions of the dust emission thus spectrally deconvolved into the two component. The map of the warm dust is almost identical to the N60 image, which can be understood by considering that the contribution of the cold dust component to the N60 band intensity is negligible as seen in the SED fitting of figure 2. The distribution of the cold dust however shows some differences from those of the other photometric band images as seen in the giant HII regions, where the contributions of the two components may be intermixed to some extent. The cold dust component seems to be smoothly distributed over

the entire extent of the galaxy, while the warm dust component indicates some correlation with the spiral arms. The cold dust may be heated by a diffuse heating source, such as an old stellar population or non-ionising UV photons escaping from HII regions. In outer regions, the warm dust component is correlated with the spotty structures that belong to the spiral arms.

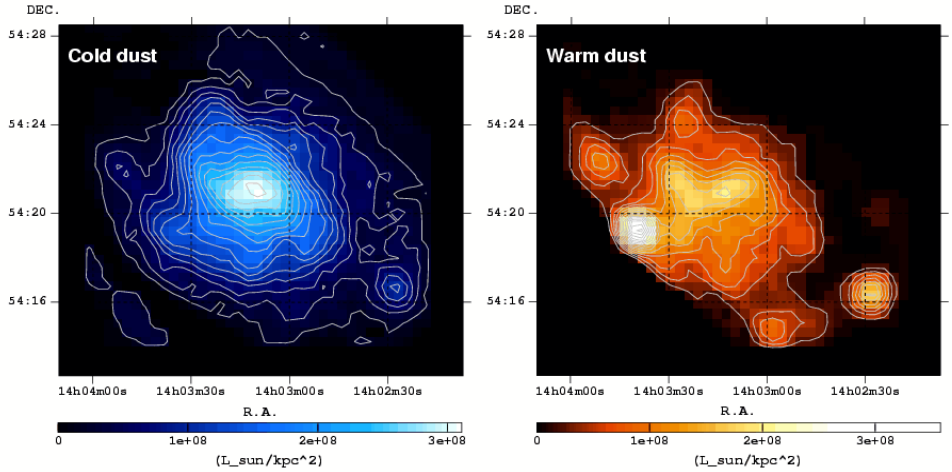

Fig. 3.— Spatial distributions of the cold dust (left), and warm dust (right) components of M101 (Suzuki et al. 2007).

On the basis of the spectrally-deconvolved dust emission maps in figure 3, we derive the far-IR luminosity ratio between warm and cold dust ($L_{\rm w}/L_{\rm c}$) in various regions, which consist of seven local fields in M101: the four giant HII regions, the center, the bar, and the inter-arm region. The results are shown in table 1. It is found from the table that the ratios of the four giant HII regions are significantly higher than those of the center and the bar, and $20-40$ times as high as that of the inter-arm region. The cold dust component is associated with gas content, while the warm dust component is associated with the SFR of massive stars. Thus, the ratio $L_{\rm w}/L_{\rm c}$ is physically related to star-formation activity. Systematic errors in the ratio are likely to be dominated by the assumption of constancy in the warm dust temperature; the dust temperature can be higher than the fixed one particularly in the giant

Table 1: Far-infrared luminosity ratio between cold and warm dust components ($L_{\rm w}/L_{\rm c}$) in various regions in M101

	Center	Bar end	NGC 5447	NGC 5455	NGC 5461	NGC 5462	Inter arm
$L_{\rm w}/L_{\rm c}$	0.6±0.1	0.8±0.2	1.6±0.4	3.0±0.7	2.6±0.6	1.9±0.4	0.07±0.02

HII regions. However, higher temperature results in larger $L_{\rm w}$, thus making the difference in $L_{\rm w}/L_{\rm c}$ between the giant HII regions and the other regions even larger. Therefore, the result in table 1 may indicate that star-formation activity of the four giant HII regions are highest in the galaxy. As a result of a past encounter of M101 with its companion galaxy, NGC 5477, intergalactic HI gas may fall in the outer disk near at least NGC 5461 and 5462 (Van der Hulst & Sancisi 1988). Therefore, such external effects may promote the formation of the giant HII regions.

4. Summary

The spatial structure of M101 is well resolved in the four bands with the AKARI/FIS. The resultant SED of the whole galaxy shows the presence of a cold dust component (18 K) in addition to a warm dust component (55 K). Considering its small $L_{\rm FIR}/M_{\rm gas}$ value of 0.9 $L_{\odot}/M_{\odot}$, M101 is classified as an inactive galaxy. We have deconvolved the cold and warm dust emission components spatially. The distribution of the cold dust is mostly concentrated near the center, and exhibits smoothly distributed over the entire extent of the galaxy, whereas the distribution of the warm dust indicates some correlation with the spiral arms, and has spotty structures such as four distinctive bright spots in the outer disk. The bright spots are spatially related to the four giant HII regions.

On the basis of the distributions of the warm and cold dust components, we have derived $L_{\rm w}/L_{\rm c}$ as a robust measure of star-formation activity in the various regions in M101. Star-formation activity of the four giant HII regions is significantly higher than that of the rest of the galaxy. Unlike our Galaxy, M101 is considered to be a peculiar normal galaxy with extraordinary active star-forming regions.

We would like to thank all the members of the AKARI project for their continuous help and support. Based on observations with AKARI, a JAXA project with the participation of ESA. We are grateful to the AKARI data reduction team for their extensive work in developing data analysis pipelines.

REFERENCES

Allen, R. J., Goss, W. M., & van Woerden, H. 1973, A&A, 29, 447.

Cox, P., & Mezger, P. G. 1989, A&A Rev., 1, 49.

De Jong, T., Clegg, P. E., Rowan-Robinson, M., Soifer, B. T., Habing, H. J., Houck, J. R., Aumann, H. H., & Raimond, E. 1984 ApJ, 278, 67.

Hippelein, H., Haas, M., Tuffs, R. J., Lemke, D., Stickel, M., Klaas, U., & Volk, H. J. 2003, A&A, 407, 137

Jurcevic, J. S., & Butcher, D. 2006, A&AS, 208, 1303.

Kawada, M. et al. 2007, PASJ, 59, 389

Kenney, J. D. P., Scoville, N. Z., & Wilson, C. D. 1991, ApJ, 366, 432.

Murakami, H. et al. 2007, PASJ, in this volume.

Nilson, P. 1973, Uppsala General Catalogue of Galaxies, Acta Universitatis Upsalienis, Nova Acta Regiae Societatis Upsaliensis, Series V: A, Vol. 1

Popescu, C. C., Tuffs, R. J., Volk, H. J., Pierini, D., & Madore, B. F. 2002, ApJ, 567, 221.

Popescu, C. C., & Tuffs R. J. 2005, AIP Conference Proceedings, 761, 155.

Sandage, A., Tammann, G. A., & van den Bergh, S. 1981, JRASC, 75, 267.

Sauvage, M. et al. 2005, in "ISO science legacy -a compact review of ISO major achievements", Space Science Reviews, eds. C. Cesarsky and A. Salama, Springer Science + Business Media, Inc., vol. 119, Issue 1-4, p. 313

Siebenmorgen, R., Krügel, E., & Chini, R. 1999, A&A, 351, 495.

Suzuki, T. et al. 2007, PASJ, 59, 473

Tuffs, R. J., & Gabriel, C. 2003, A&A, 410, 1075.

Van der Hulst, T., & Sancisi, R. 1988, AJ, 95, 135.

Vlahakis, C., Dunne, L., Eales, S. 2005, MNRAS, 364, 1253.